Neurobiology of Disease

Multiple Factors Contribute to the Peripheral Induction of Cerebral β-Amyloidosis

Yvonne S. Eisele,[1,3]* Sarah K. Fritschi,[1,2,3]* Tsuyoshi Hamaguchi,[1]* Ulrike Obermüller,[1,3] Petra Füger,[1,3] Angelos Skodras,[1,3] Claudia Schäfer,[1,3] Jörg Odenthal,[1,3] Mathias Heikenwalder,[4] Matthias Staufenbiel,[1,3] and Mathias Jucker[1,3]

[1]Department of Cellular Neurology, Hertie Institute for Clinical Brain Research, University of Tübingen, D-72076 Tübingen, Germany, [2]Graduate School of Cellular and Molecular Neuroscience, University of Tübingen, D-72074 Tübingen, Germany, [3]German Center for Neurodegenerative Diseases, D-72076 Tübingen, Germany, and [4]Institute for Virology, Technische Universität München/Helmholtz Zentrum München, D-81675 Munich, Germany

Deposition of aggregated amyloid-β (Aβ) peptide in brain is an early event and hallmark pathology of Alzheimer's disease and cerebral Aβ angiopathy. Experimental evidence supports the concept that Aβ multimers can act as seeds and structurally corrupt other Aβ peptides by a self-propagating mechanism. Here we compare the induction of cerebral β-amyloidosis by intraperitoneal applications of Aβ-containing brain extracts in three Aβ-precursor protein (APP) transgenic mouse lines that differ in levels of transgene expression in brain and periphery (APP23 mice, APP23 mice lacking murine APP, and R1.40 mice). Results revealed that beta-amyloidosis induction, which could be blocked with an anti-Aβ antibody, was dependent on the amount of inoculated brain extract and on the level of APP/Aβ expression in the brain but not in the periphery. The induced Aβ deposits in brain occurred in a characteristic pattern consistent with the entry of Aβ seeds at multiple brain locations. Intraperitoneally injected Aβ could be detected in blood monocytes and some peripheral tissues (liver, spleen) up to 30 d after the injection but escaped histological and biochemical detection thereafter. These results suggest that intraperitoneally inoculated Aβ seeds are transported from the periphery to the brain in which corruptive templating of host Aβ occurs at multiple sites, most efficiently in regions with high availability of soluble Aβ.

Key words: **Abeta; cerebral beta-amyloidosis; peripheral induction; seeding**

Introduction

Cerebral β-amyloidosis, a hallmark of Alzheimer's disease (AD), can be exogenously induced by the intracerebral infusion of β-amyloid (Aβ) containing brain extracts into young Aβ-precursor protein (APP) transgenic (Tg) mice (Kane et al., 2000; Meyer-Luehmann et al., 2006; Eisele et al., 2009; Watts et al., 2011; Hamaguchi et al., 2012; Morales et al., 2012; Rosen et al., 2012). The beta-amyloidosis inducing activity has been shown to consist of multimeric Aβ peptides (Meyer-Luehmann et al., 2006). Subsequent studies have demonstrated that aggregated synthetic Aβ is itself sufficient to induce cerebral β-amyloidosis although with lower biological activity than the Aβ-containing brain extracts (Stöhr et al., 2012). These observations are reminiscent of prion disorders such as Creutzfeldt-Jakob disease or bovine spongiform encephalitis in which it is now established beyond a reasonable doubt that these disorders can be transmitted by exogenous, conformational variants of the prion protein (PrP; Colby and Prusiner, 2011). It is currently hypothesized that the self-replication of pathogenic protein aggregates (prion-like misfolding of proteins) is a uniform principle responsible for the instigation and spreading of many age-related neurodegenerative disorders (Jucker and Walker, 2013).

We found previously that intraperitoneal applications of Aβ-containing brain extract can also induce cerebral β-amyloidosis in young APP23 Tg mice, albeit at a higher concentration and a longer incubation interval compared to the intracerebral inoculation route (Eisele et al., 2010). In APP23 Tg mice, expression of human APP is primarily confined to neurons in the brain (Sturchler-Pierrat et al., 1997), but murine APP is also expressed in peripheral neuronal and non-neuronal tissues and may contribute to peripheral seeding. From studies in the prion field, it is known that the cellular PrP (PrP^{C}) in peripheral cells plays a crucial role in the transfer of the infectious prion (PrP^{Sc}) from the periphery to the CNS (Blättler et al., 1997), and PrP^{Sc} accumulates in some peripheral sites, such as lymphoid tissues, during its transmission from the periphery to the brain (Mabbott and MacPherson, 2006; Aguzzi et al., 2013).

Received April 19, 2014; revised June 9, 2014; accepted June 17, 2014.

Author contributions: Y.S.E., S.K.F., T.H., M.S., and M.J. designed research; Y.S.E., S.K.F., T.H., U.O., and C.S. performed research; J.O. and M.H. contributed unpublished reagents/analytic tools; Y.S.E., S.K.F., T.H., P.F., A.S., and M.J. analyzed data; Y.S.E., S.K.F., M.S., and M.J. wrote the paper.

This work was supported by grants from the Competence Network on Degenerative Dementias (BMBF-01GI0705) and the BMBF as part of ERA-Net NEURON (MIPROTRAN). T.H. was supported by a postdoctoral fellowship from the Humboldt foundation. We thank Lary Walker (Atlanta, GA) and Frank Baumann (Tübingen, Germany) for comments on this manuscript, Stephan Käser, Götz Heilbronner, Judith Finkbeiner, Anika Bühler, Stefan Grathwohl, and Nick Varvel (Tübingen, Germany) for the help with the immunoassays and immunostaining, and all the other members of our laboratory for their contributions. The generous donation of the pFTAA dye from Peter Nilsson (Linköping, Sweden) is greatly appreciated. The advice and help of Bruce Lamb with the R1.40 mice is greatly acknowledged.

*Y.S.E., S.K.F., and T.H. contributed equally to this work.

Correspondence should be addressed to either Yvonne S. Eisele or Mathias Jucker at the above address. E-mail: yvonne.s.eisele@gmail.com or mathias.jucker@uni-tuebingen.de.

DOI:10.1523/JNEUROSCI.1608-14.2014

 0270-6474/14/3410264-10$15.00/0

In the present study, we characterize the nature, mechanism, and the time- and concentration-dependent intraperitoneal induction of cerebral β-amyloidosis. We compare APP23 mice as hosts with a second Tg mouse strain, R1.40, that harbors a yeast artificial chromosome containing a genomic copy of the human APP gene. In R1.40 mice, human APP is expressed not only in the brain but also in the systemic organs, such as kidney, testes, and heart, and reflects normal tissue-specific APP/Aβ expression (Lamb et al., 1997). As a complementary host system, we used APP23 mice bred on a murine *App*-null background (Calhoun et al., 1999), i.e., a host expressing only human APP in brain and devoid of peripheral APP expression. The present study confirms the concept of prion-like misfolding of Aβ and suggests that Aβ seeds can be transported from distant locations to the brain in which corruptive templating of host Aβ occurs.

Materials and Methods

Mice. APP23 Tg mice (Sturchler-Pierrat et al., 1997) expressing a human APP751 cDNA with the K670N–M671L mutation under control of the murine Thy1.2 promoter were backcrossed with C57BL/6J mice for >20 generations and maintained on a C57BL/6J background [C57BL/6J-Tg(Thy1–APPK670N;M671L)]. To generate APP23 mice on a murine *App*-null background, hemizygous APP23 mice were bred with C57BL/6J–*App* mice (Calhoun et al., 1999). The resulting APP23/$App^{+/-}$ mice were bred with APP23/$App^{+/-}$ to obtain the desired APP23/$App^{-/-}$ line. Hemizygous R1.40 APP Tg mice on a B6.129 background were purchased from The Jackson Laboratory. The mice carry a yeast artificial chromosome containing the genomic copy of human APP harboring the K670N–M671L mutation (Lamb et al., 1997). The mice were bred once with C57BL/6J mice; then homozygous R1.40 mice were generated by crossbreedings, resulting in homozygous mice on a B6.129/C57BL/6J background. C57BL/6J mice were purchased from The Jackson Laboratory. All inoculations in the present study were done with homozygous R1.40 mice and hemizygous APP23 mice. Female and male mice were used in all experiments with the exception of the results presented in Figure 3 for which only male mice were used. When males and females were used, care was taken that groups had a similar number of males and females. As indicated in the individual figure legends, male and female mice were combined because either statistical analysis did not reveal a significant difference or numbers were too small to do proper statistical gender analysis. Overall, the induction of amyloid appeared somewhat higher in females compared with males. All mice were maintained under specific pathogen-free conditions. The experimental procedures were undertaken in accordance with the veterinary office regulations of Baden-Württemberg (Germany) and approved by the local animal care and use committees.

Brain tissue extracts. Brains from aged (18–30 months old) male and female Tg APP23 and APPPS1 donor mice or age-matched, non-Tg [wild-type (WT)] mice of our APP23 or APPPS1 colonies were used (Sturchler-Pierrat et al., 1997; Radde et al., 2006). After the cerebellum and lower brainstem were removed, the forebrains were frozen on dry ice and stored at −80°C. Brains were individually homogenized at 10% (w/v) in sterile PBS (Lonza), vortexed, sonicated three times for 5 s (Lab Sonic; B. Braun; 0.5-mm-diameter sonotrode, cycle 1, amplitude 80%) and centrifuged at 3000 × *g* for 5 min. The supernatant was aliquoted and stored at −80°C until use. Aβ levels in extracts prepared from individual brains were determined using electrochemiluminescence-linked immunoassay and/or immunoblotting as described previously and revealed total Aβ concentrations of 10–20 ng/μl in the Tg extract (Eisele et al., 2009). Aliquots of several extracts (from at least three animals, Tg or WT, respectively) were thawed just before intraperitoneal injections and mixed to yield large batches of Tg or WT seeding extracts. All injected extracts were derived from aged APP23 Tg mice but occasionally also contained a minor amount (<10% v/v) of extract derived from aged APPPS1 Tg mice. [Note that adding such a minor amount of APPPS1 extract was shown to yield similar induction of cerebral β-amyloidosis as pure APP23 seeding extract in APP23 Tg mice (Eisele et al., 2010) and has no major influence on the $A\beta_{40}/A\beta_{42}$ ratio of the seeding extract mix.]

Intraperitoneal inoculation. Mice received two intraperitoneal injections of 100 μl of Tg extract or WT extract 1 week apart, unless indicated otherwise. For the concentration-dependent study, mice received a single intraperitoneal injection of 200 μl of Tg extract or 1:10, 1:100, or 1:1000 PBS dilutions thereof. All mice were randomly assigned to the inoculation groups.

Mixture of anti-Aβ antibodies and Tg brain extract. Before the intraperitoneal inoculation, Tg extract was 2:1 mixed with 4.5 mg/ml of the anti-Aβ antibody β1 (monoclonal, mouse IgG2a; Meyer-Luehmann et al., 2006). The mixing procedure results in a 6.7% extract. A total of 200 μl of this mixture was intraperitoneally injected into APP23 hosts.

Preparation of inoculated mice. APP23 Tg mice were prepared 1, 4, 6, 7, and 8 months after inoculation without perfusion. APP23 Tg mice on an *App*-null background (APP23/$App^{-/-}$) were prepared 8 months after inoculation. Brains were removed, and right hemispheres were directly frozen on dry ice for biochemical analysis and stored at −80°C. Left hemispheres were immersion fixed in 4% paraformaldehyde in PBS for 48 h, cryoprotected in 30% sucrose, frozen in 2-methylbutane, and stored at −80°C until analysis. R1.40 mice, which normally develop Aβ pathology later in life than do APP23 mice (Hamaguchi et al., 2012), were prepared 1, 6, 8, 10, and 12 months after intraperitoneal injections. R1.40 mice were killed under deep ketamine/xylazine anesthesia (400 mg/kg ketamine, 40 mg/kg xylazine) and transcardially perfused with PBS. The brains were harvested and hemi-dissected. Right hemispheres were again directly frozen, and the left hemispheres were immersion fixed. Peripheral organs were also taken when indicated and immersion fixed in 4% paraformaldehyde, followed by paraffin embedding.

Histology and immunohistochemistry. Fixed frozen brains were cut into 25-μm-thick coronal sections using a freezing-sliding microtome. Paraffin-embedded tissue was cut into 6-μm-thick sections on a rotary microtome (Microm HM 325), and a previously published enhanced antigen retrieval technique was used (Kai et al., 2012). All sections were Aβ immunostained using polyclonal antibody CN3 (1:1000; raised against residues 1–16 of human Aβ; Eisele et al., 2010) and visualized using standard immunoperoxidase procedures with the Vectastain Elite ABC kit (Vector Laboratories). After immunohistochemistry, some sections were additionally stained with Congo red and visualized between cross-polarizers and/or counterstained with nuclear fast red. To analyze the integrity of the blood–brain barrier, sections were immunostained with antibodies against mouse IgG (1:250; Vector Laboratories) and mouse albumin (rabbit polyclonal, 1:1000; Thermo Fisher Scientific). Visualization was done as described above. The Prussian blue histological stain with nuclear fast red counterstaining was used to visualize ferric iron in hemosiderin and performed as described previously (Winkler et al., 2001).

Immunoblot and immunoassay for APP and Aβ. Right brain hemispheres were homogenized at 10% (w/v) in homogenization buffer [in mM: 50 Tris, pH 8.0, 150 NaCl, 5 EDTA, and Complete Mini protease inhibitor mixture (Roche)]. To assess Aβ and APP levels, 4–12% NuPage Bis-Tris mini gels using NuPage LDS sample buffer were used (Invitrogen), followed by protein transfer onto nitrocellulose membranes and probing with antibody 6E10 (Covance). Monoclonal anti-GAPDH antibody (Hy Test) was used to detect the housekeeping protein GAPDH. Densitometric values of band intensities were analyzed using NIH ImageJ 1.44 (http://rsbweb.nih.gov/ij/).

For electrochemiluminescence-conjugated immunoassay, 500 μl of homogenized brain sample (10% w/v in PBS) was extracted with an equivalent volume of 0.4% diethylamine (DEA) and centrifuged at 135,000 × *g* for 1 h at 4°C. A total of 850 μl of the supernatant was neutralized with 85 μl of 0.5 M Tris-HCl, pH 6.8, to obtain the DEA-soluble fraction. The DEA-insoluble pellet was resuspended to 500 μl volume with 70% formic acid (FA), incubated at 4°C for 12 h, and then sonicated for 35 s at 4°C. The samples were analyzed on a Sector Imager 6000 using the MSD 96-well Multi-Spot Human 6E10 Aβ Triplex Assay (Meso Scale Discovery).

Quantification of Aβ load on brain sections. The areal density of Aβ-immunoreactive lesions (CN3 staining) and Congo red staining was

Table 1. Classification of plaque size according to area on section

Area (μm^2)	Minimum circular diameter (μm^2)	Class
$A > 14000$	133.5	Large
$14000 \geq A > 4000$	71.4	Medium
$4000 \geq A > 800$	31.9	Small
$800 \geq A \geq 20$	5.04	Very small
$A < 20$		Excluded

A, Area.

quantified in random-systematic sets through the neocortex according to four categories: (1) CN3-positive vascular; (2) CN3-positive parenchymal; (3) Congo red-positive vascular; or (4) Congo red-positive parenchymal. For APP23 Tg and APP23/*App*$^{-/-}$ mice, every 24th section was assessed. The Aβ load (% Aβ-immunostained area) of R1.40 Tg mice was lower compared with the APP23 mice, and thus every 12th section was assessed. Stereological analysis was performed using a Zeiss Axioskop microscope equipped with a motorized *x–y–z* stage coupled to a video-microscopy system and the Stereo Investigator software (MicroBrightField). Quantification was performed by researchers who were blinded to the inoculation groups.

Distance distribution analysis of parenchymal amyloid plaques. Mosaic images of entire brain sections were acquired with a Zeiss Axioplan Microscope (MosaiX module, Zeiss AxioVision software) and imported in Fiji (http://fiji.sc/Fiji). A systematically sampled set of every 12th coronal section throughout the brain was imaged and analyzed as described previously (in total ~12 sections per animal).

A macro was written in Fiji to automate plaque recognition in a user-selected region of interest (ROI). An experienced scientist manually selected the ROI corresponding to the cerebral cortex, and care was taken to exclude ambiguous structures and vascular amyloid from the ROI. CN3-stained plaques were segmented using the luminance of the imported image (L channel of the CIELAB color space, readily available in Fiji as a plugin) and applying the RATS (Robust Automated Thresholding Selection) plugin available in Fiji (Wilkinson, 1998). In addition, the watershed transformation was used to split touching objects, improving the plaque segmentation. After completion, the area of each plaque in square micrometers was obtained, as well as its *x–y* centroid coordinates and major and minor axes of a fitted ellipse. The plaques were assumed to have a circular profile, the diameter of which was obtained by averaging the sum of the major and minor axes of the fitted ellipse. The assumption of the circular shape was empirically confirmed not to have an effect on the overall results of the analysis.

Pairwise two-dimensional Euclidean distances were calculated between the surface of each plaque and every other plaque in the ROI, using the *x–y* coordinates and the circular diameter obtained by the image recognition macro:

$$d_{ij} = \sqrt{(x_i - x_j)^2 + (y_i - y_j)^2} - r_i - r_j,$$

where d_{ij} indicates the surface-to-surface distance between two plaques, *i* and *j*, plaque *i* has center coordinates (x_i, y_i) and circular diameter r_i. The calculations were performed using a program written in Fortran 77. The program calculates the number of neighbors within set distances of the plaque surface, for each plaque, based on the Euclidean distances (above equation), to quantify the local spatial arrangement of the structures of interest (Hefendehl et al., 2014).

To investigate the number of small amyloid deposits around plaques of various sizes, identified plaques were empirically assigned to four categories, according to their area on the section (Table 1; see Fig. 4). Plaques that had an area smaller than 20 μm^2, corresponding to a diameter of ~5 μm, were excluded from the analysis.

Peritoneal lavage. Peritoneal monocytes/macrophages were isolated by peritoneal lavage of two 5 ml doses of ice-cold PBS at the time the animals were killed. The recovered cell suspension was put on ice, and the cells were isolated by centrifugation (300 × *g* for 5 min; Kim et al., 1997). The cell pellet was resuspended in PBS for additional analysis.

Blood collection. EDTA-anticoagulated whole-blood samples were taken by cardiac puncture at the time the animals were killed. For electrochemiluminescence-linked immunoassays and immunoblotting, the blood samples were separated into plasma and the cellular pellet by centrifugation for 5 min at 16,000 × *g* at room temperature. The blood pellets were resuspended in the plasma-equivalent volumes of 1× homogenization buffer [in mM: 50 Tris, pH 8.0, 150 NaCl, 5 EDTA, and Complete Mini protease inhibitor (Roche)]. Samples were snap frozen and stored at −80°C until analysis.

Aβ quantification in blood. For electrochemiluminescence-linked immunoassay, blood plasma was subjected to measurement without additional treatment. The resuspended blood pellet (see above) containing the cellular components was treated with FA (minimum of 95%), sonicated for 35 s on ice, and centrifuged at 25,000 × *g* for 1 h at 4°C. Supernatants were neutralized (1 M Tris base, 0.5 M Na_2HPO_4, and 0.05% NaN_3). Aβ levels were determined in duplicates using the MSD 96-well MULTI-ARRAY Human (6E10) $A\beta_{40}$ and $A\beta_{42}$ Ultra-Sensitive Assay or MULTI-SPOT Human (6E10) Aβ Triplex Assay (Meso Scale Discovery) and read on a Sector Imager 6000 according to the instructions of the manufacturer. Each sample was measured twice, and the mean was taken. Levels below detection (depending on the experiment; ~5 pg/ml) were taken as zero. Resuspended cells isolated by peritoneal lavage were likewise subjected to FA treatment. For Aβ detection by immunoblotting, the resuspended blood pellet was subjected to immunoprecipitation using anti-Aβ antibody 6E10 (Covance) and Dynal paramagnetic beads with sheep anti-mouse IgG (Invitrogen) as described previously (Meyer-Luehmann et al., 2006).

Histochemical and immunohistochemical staining of cells from the blood and peritoneal cavity. Blood films on Superfrost slides (R. Langenbrink, Emmendingen, Germany) were air dried for 24 h at room temperature. Cells were fixed using methanol/acetone (1:1) for 90 s and air dried again. Cells obtained by peritoneal lavage were resuspended in PBS and subjected to cytospin (Cytospin J; Thermo Shandon) using disposable single cell funnels (JC320; Tharmac). Pappenheim's stain (Giemsa's solution, May-Grünwald's solution; Merck) was used for the differentiation of cells isolated from the blood and peritoneal cavity. For immunohistochemical analysis, slides were preincubated in PBS containing 0.1% Triton X-100 (Sigma). In combination with Pappenheim's stain, Aβ immunostaining (CN3 antibody) was performed using standard immunoperoxidase procedures with the Vectastain Elite ABC kit (Vector Laboratories). Double labeling for Aβ (CN3 antibody) and CD11b, CD45, or CD68 (Serotec) was performed using standard immunofluorescence procedures with goat anti-rabbit Alexa Fluor 568 and goat anti-rat Alexa Fluor 488 secondary antibodies (Invitrogen). For staining with pFTAA [pentamer formyl thiophene acetic acid (sodium salt), part of the amyloid-binding class of luminescent conjugated oligothiophene (LCO) dyes; Klingstedt et al., 2011], cytospins from peritoneal lavage were dried at room temperature for 2 h and incubated with PBS for 10 min. Staining with pFTAA (1.5 mM in deionized water, diluted 1:1000 in PBS) was performed as described previously (Klingstedt et al., 2011). The sections were mounted with Vectashield mounting medium for fluorescence with DAPI (Vector Laboratories). Images were acquired on a Zeiss LSM 510Meta laser scanning confocal microscope using a 63×/1.4 numerical aperture oil-immersion objective (Axiovert 200M; Zeiss). The amyloid-binding dye pFTAA was excited with the 488 nm laser line, and its emission was collected in the range of 505–550 nm. The dyes were imaged sequentially.

Statistical analysis. All values are expressed as means ± SEMs. The statistical analyses were performed using GraphPadPrism (version 6.0) and/or JMP 8, and results are detailed in the figure legends.

Results

Earlier and stronger amyloid induction in APP23 compared with R1.40 Tg mice

APP23 and R1.40 mice at the age of 1–2 months were inoculated with the same brain extracts derived from either aged non-Tg WT mice (WT extract) or Aβ bearing brain extract derived from APP23 and APPPS1 Tg mice (the extracts of the individual mice were pooled; see Materials and Methods; Tg extract). All mice received two intraperitoneal injections of 100 μl each 1 week

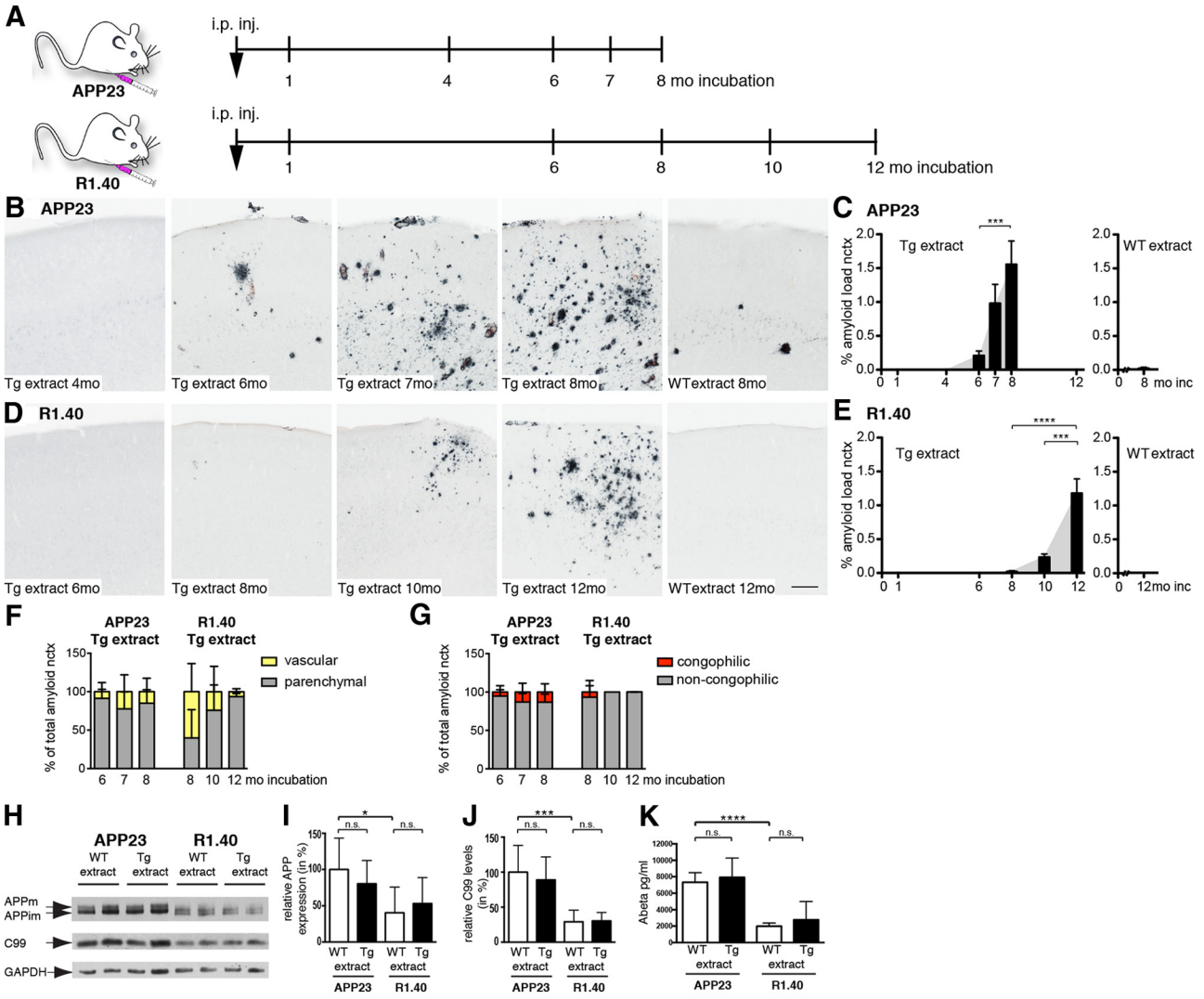

Figure 1. Time course reveals earlier and stronger induction of cerebral β-amyloidosis in APP23 versus R1.40 Tg mice with the same peripherally applied Aβ-containing seeding extract. ***A***, Experimental design: 1- to 2-month-old male and female APP23 and R1.40 Tg mice were intraperitoneally injected (i.p. inj.; two times with 100 μl, 1 week apart) with brain extracts derived from either aged non-Tg mice (WT extract) or aged Aβ-depositing APP Tg mice (Tg extract). Brains of inoculated APP23 mice were analyzed 1, 4, 6, 7, and 8 months and brains of inoculated R1.40 mice at 1, 6, 8, 10, and 12 months after inoculation [incubation (inc.)]. Male and female mice were combined for the analysis (see Material and Methods). ***B–E***, Immunohistochemical analysis for Aβ deposition. ***B***, In intraperitoneally inoculated APP23 mice, the first Aβ deposits were noted at 6 months and increased sharply with the longer incubation times of 7 or 8 months. In contrast, mice that received the WT extract and were incubated for 8 months showed no or very few Aβ deposits, which are typical for APP23 Tg mice at 8–10 months of age, which is the age at analysis. Stereological quantification of neocortical Aβ load is shown in ***C***. In R1.40 Tg mice, the first Aβ deposits occurred 8 months after inoculation in all mice that received the Tg extract albeit to a minor extent and increases with longer incubation times of 10 or 12 months. In contrast, mice that received the WT extract showed no or very little Aβ deposits after a 12 month incubation (***D***) that is a typical finding for R1.40 Tg mice at 10–14 months of age, which is the age at analysis. Stereological quantification of neocortical Aβ load is shown in ***E***. $n = 5–9$ for APP23 and R1.40 Tg mice per incubation time and extract; $^{***}p < 0.001$, $^{****}p < 0.0001$, one-way ANOVA, Bonferroni's *post hoc* test. Scale bar, 200 μm. ***F***, Neocortical Aβ deposits in both lines were further differentiated into vascular and parenchymal deposits, and results revealed that, in APP23 Tg mice, the majority of deposits (measured by area occupied) are parenchymal deposits with a high variability for vascular deposits. Interestingly, in R1.40 mice, vascular deposition seemed prominent during early time points but decreased thereafter and parenchymal deposits became more dominant. ***G***, Differentiation of the neocortical Aβ deposits into congophilic (Congo red positive) and non-congophilic deposits revealed that, in APP23 Tg mice, 5–15% of induced deposits are congophilic, whereas in R1.40 mice, almost exclusively diffuse deposits are induced at least up to 12 months incubation. (However, note that Congo red stains only the core of a plaque and thus the area fraction is low compared with the Aβ stain of a given amyloid plaque.) ***H–K***, Biochemical analysis of brains 1 month after inoculation. Representative immunoblot for APP, differentiated into mature APP (APPm) and immature APP (APPim) as well as C99 levels, both recognized by the 6E10 antibody specific to human APP (***H***). Relative APP levels (APPm and APPim combined) were quantified from immunoblots and normalized to the housekeeping protein GAPDH. Mean APP value for WT extract-injected APP23 Tg mice was set to 100%. Quantification shows no difference between APP23 mice injected with WT or Tg extract. Similarly, no difference was found in R1.40 mice. However, APP levels in R1.40 Tg mice were lower than in APP23 Tg mice representing ~30% of APP levels of APP23 mice (***I***). Overall, similar results were found for C99 levels (***J***). Human Aβ levels in brain homogenates were assessed with electrochemiluminescence-linked immunoassay, and again, similar to APP and C99 levels, human Aβ levels did not differ between mice of the same Tg line treated with either WT or Tg brain extract. Between the two lines, human Aβ levels in APP23 mice are significantly higher and are approximately threefold to fourfold in APP23 compared with R1.40 mice (***K***). $n = 8$ for APP23; $n = 5$ for R1.40. Note that the same animals (1 month incubation) were used for biochemical analysis and histology. $^{*}p < 0.05$, $^{***}p < 0.001$, $^{****}p < 0.0001$, one-way ANOVA, Sidak's multiple comparison test. nctx, Neocortex.

apart. For each mouse line, five different time points were chosen for the analysis: 1, 4, 6, 7, and 8 months after inoculation for APP23 mice and 1, 6, 8, 10, and 12 months for R1.40 Tg mice (Fig. 1*A*). For the APP23 line, the time points were chosen based on our previous work in which we found induction of cerebral β-amyloidosis after 6–7 months in this line (Eisele et al., 2010). For R1.40 mice, we found in pilot experiments (data not shown) that amyloid induction after intraperitoneal inoc-

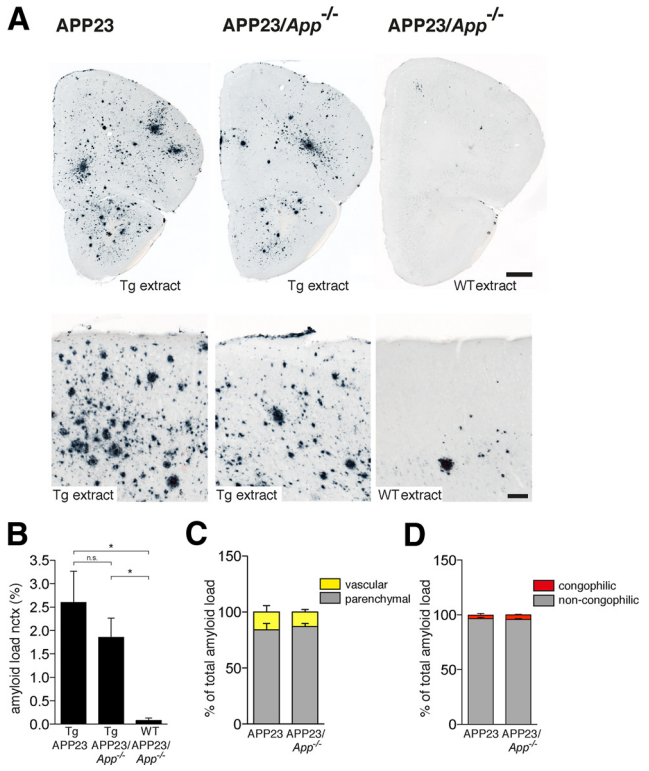

Figure 2. Induction of cerebral β-amyloidosis by intraperitoneal seeding in the absence of peripheral APP expression. ***A***, Male and female APP23 mice and APP23 mice on an *App*-null background (APP23/*App*$^{-/-}$; all 1–2 months of age) were intraperitoneally inoculated with 200 μl of brain extract from aged Aβ-depositing APP23 mice (Tg extract) or non-Tg WT mice (WT extract) and analyzed for cerebral Aβ deposition 8 months later. Male and female mice were combined for the analysis (see Material and Methods). Shown are representative coronal sections (scale bar, 500 μm), and higher-magnification images of the frontal cortex are shown below (scale bar, 100 μm). Immunohistochemical analysis revealed a similar, albeit somewhat lower, induction of Aβ deposition by the Tg extract in APP23/*App*$^{-/-}$ mice compared with the APP23 mice. Mice that received the WT extract showed no induced Aβ deposits. Note that 9- to 10-month-old APP23 and APP23/*App*$^{-/-}$ mice (age at preparation) do exhibit the first endogenous Aβ deposition at this age. ***B***, Stereological quantification indeed revealed that the amyloid load of APP23/*App*$^{-/-}$ was 29% less compared with APP23 mice, but the difference did not achieve significance ($n = 4$ for APP23 mice and APP23/*App*$^{-/-}$ mice injected with WT extract and $n = 8$ for APP23/*App*$^{-/-}$ inoculated with Tg extract; mean ± SEM; one way ANOVA, $F_{(2,13)} = 6.136$, $p = 0.013$, Tukey's multiple comparison, $^{*}p < 0.05$; n.s., not significant). ***C***, Neocortical Aβ load was differentiated into vascular and parenchymal deposits. No difference was noted between APP23 and APP23/*App*$^{-/-}$ mice. ***D***, Differentiation of neocortical amyloid in congophilic (Congo red positive) and non-congophilic Aβ lesions also revealed a similar distribution of deposits in both APP23 and APP23/*App*$^{-/-}$ Tg mice. nctx, Neocortex.

ulation is only scarce after 8 months, and thus longer time points were chosen.

For the inoculated APP23 mice, no induced Aβ deposits in brain were found at 1 and 4 months after inoculation. However, robust induction of cerebral β-amyloidosis with the Tg extract was found 6 months after inoculation with a time-dependent increase thereafter (Fig. 1*B*,*C*). Notably, WT extract did not induce cerebral β-amyloidosis at any time points (Fig. 1*C*). In the intraperitoneally inoculated R1.40 mice, cerebral β-amyloidosis was detectable for the first time at 8 months after inoculation with the Tg extract and further increased with longer incubation times (Fig. 1*D*,*E*). Similar to APP23 hosts, WT extract did not induce Aβ deposits in R1.40 mice (Fig. 1*E*). Although the histological quantification revealed 1.3-fold more induced Aβ deposition in the APP23 host (after the 8 months incubation) compared with the R1.40 host (after the 12 months incubation; Fig. 1*C*,*E*), a quantitative immunoassay detected 45-fold more insoluble Aβ ($Aβ_{40}$ and $Aβ_{42}$ combined) in the inoculated APP23 compared with the inoculated R1.40 mice [2877.9 ± 473.0 vs 61.6 ± 14.6 ng/ml 10% (w/v) brain homogenate]. The apparent discrepancy is likely related to the essentially diffuse nature of the induced deposits in the R1.40 mouse line, whereas the induced Aβ deposits in the APP23 host were more frequently compact and congophilic (Fig. 1*G*).

In addition to parenchymal deposits, vascular Aβ deposits were induced in both lines (Fig. 1*F*). Although the relative percentage of induced amyloid around the vasculature was greatest at early time points in the R1.40 mice and decreased thereafter, this observation was not evident for the APP23 mice in the present experiment, in contrast to our previous study (Eisele et al., 2010). Interestingly, both lines showed prominent and early Aβ deposits in leptomeningeal vessels when inoculated with the Tg extract in contrast to inoculations with WT extract in which such deposits were absent.

We next analyzed human APP levels and APP processing 1 month after inoculation in APP23 and R1.40 mice to assess potential short-term effects of intraperitoneal inoculations with the Tg extract compared with the WT extract. Moreover, this allowed for a direct comparison of human (Tg) APP protein expression in both lines and thus may explain the different seeding efficacies between the two host lines. Immunoblot analysis revealed no difference in APP levels or levels of its C99 fragment between Tg- and WT-inoculated mice for both mouse lines (Fig. 1*H*). When comparing APP23 with R1.40 Tg mice, APP and C99 levels were twofold to threefold higher in APP23 Tg mice compared with R1.40 mice (Fig. 1*I*,*J*). This is in line with the previous work reporting a fivefold to sevenfold overexpression of human APP over murine APP in hemizygous APP23 Tg mice (Sturchler-Pierrat et al., 1997) and a twofold to threefold overexpression of human versus murine APP in homozygous R1.40 Tg mice (Lamb et al., 1997). Consistent with the expression of APP and C99, an immunoassay did not reveal any difference in "total" Aβ (here defined as $Aβ_{40}$ plus $Aβ_{42}$) between WT and Tg extract inoculated APP23 or R1.40 mice at this early time point (Fig. 1*K*). In comparison, human Aβ levels in APP23 Tg mice were approximately threefold higher than in R1.40 Tg mice, paralleling the difference in APP and C99 levels (Fig. 1*K*). These results suggest that the stronger amyloid induction in APP23 compared with R1.40 mice after intraperitoneal inoculation with the same Aβ-containing brain extract is related to the higher APP overexpression and higher Aβ levels in APP23 brains.

To exclude that blood–brain barrier disruption was responsible for the observed phenomenon, we next analyzed whether we could detect mouse IgG, mouse albumin, or microhemorrhages in brains of intraperitoneally seeded APP23 and R1.40 mice. Results did not reveal evidence for blood–brain barrier damage at any of the investigated time points after intraperitoneal inoculation, with the exception of albumin staining associated with the induced (congophilic) amyloid deposits. However, the latter also prominently occurs in aged APP23 mice and to a lesser extent in aged R1.40 mice because most of the amyloid deposits in R1.40 mice are of a diffuse nature (data not shown).

Cerebral beta-amyloidosis induction does not require peripheral APP expression

Both Tg mouse lines used express endogenous murine APP in brain and in the periphery (R1.40 additionally express peripheral human APP). To study a possible effect of peripheral APP/Aβ on

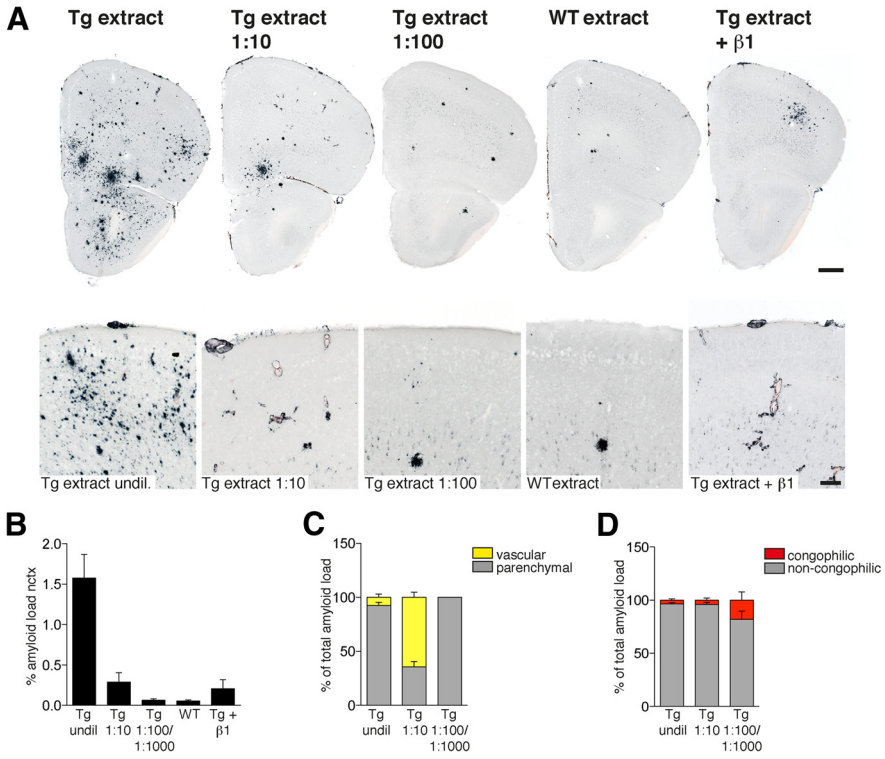

Figure 3. Concentration-dependent induction of cerebral β-amyloidosis by intraperitoneal seeding with Aβ-containing brain extract in APP23 mice. ***A***, Tg extract and PBS dilutions 1:10 and 1:100 thereof (200 μl) were intraperitoneally injected into young 1- to 2-month-old APP23 mice. Control mice were inoculated with 200 μl of brain extract from non-Tg WT mice (WT extract). The last group received a Tg extract that was mixed with the anti-Aβ-specific antibody β1 before the injection. All mice were males. Brains were immunohistochemically analyzed for Aβ deposition 8 months after intraperitoneal injection. Shown are representative coronal sections (scale bar, 500 μm), and higher-magnification images of the frontal cortex are shown below (scale bar, 100 μm). The undiluted Tg extract induced the expected Aβ deposition (see also Fig. 1*B*). The 1:10 diluted Tg extract induced appreciable amyloid deposition, whereas the 1:100 diluted Tg extract did no longer induce noticeable Aβ deposits (the same was true for the 1:1000 dilution; data not shown) and was identical to the WT extract-injected mice. Amyloid deposition in mice that received the extract/β1 mixture was markedly reduced. Note that some endogenous Aβ plaques are typical for 9- to 10-month-old APP23 mice (age at analysis). ***B***, Stereological quantification of neocortical Aβ load, $n = 3–4$ mice per group; for the analysis, the 1:100 and 1:1000 dilutions were combined; mean ± SEM is indicated). ***C***, Neocortical Aβ load was differentiated into vascular and parenchymal deposits. Although the majority of Aβ deposits induced by the undiluted Tg extract were detected in the brain parenchyma, deposition induced by the 1:10 diluted Tg extract showed prominent percentage of vascular deposits. ***D***, Neocortical amyloid load was differentiated in congophilic (Congo red positive) and non-congophilic Aβ deposits revealing that the induced Aβ deposits are primarily of a diffuse nature. (However, note that Congo red stains only the core of a plaque and thus the area fraction is low compared with the Aβ stain of a given amyloid plaque.) The increased percentage of Congo red staining in the 1:100 dilution group represents the endogenous Aβ plaques. nctx, Neocortex; undil, undiluted.

cerebral amyloid induction, APP23 mice and APP23 on a murine *App*-null background (APP23/$App^{-/-}$) were peripherally injected with Tg extract and analyzed 8 months after inoculation (Fig. 2). Results revealed qualitatively similar neocortical amyloid induction in both mouse lines (Fig. 2*A*,*B*). Quantitative analysis indicated that the induction in the APP23 host lacking murine APP was 29% lower compared with the induction in the APP23 host, although this difference was not significant (Fig. 2*C*). Because virtually the same difference (25%) in endogenous cerebral β-amyloidosis (measured as percentage Aβ-immunostained area as assessed in the present study) between APP23 and APP23 on a murine *App*-null background was found (J. Mahler, B. M. Wegenast-Braun, J. Morales-Corraliza, P. Mathews, and M. Jucker, unpublished observations), this indicates that higher amyloid load in APP23 Tg mice is likely attributable to murine Aβ co-depositing with human Aβ in the brain. The present observations in APP23 Tg mice on *App*-null background indicate that peripheral APP/Aβ is not required for the intraperitoneal induction of cerebral β-amyloidosis.

Concentration-dependent induction of cerebral β-amyloidosis and efficient blocking with anti-Aβ antibody

Although our standard inoculation protocol consisted of two injections of 100 μl of brain extract given 1 week apart, we wondered whether a single inoculation of 200 μl of Tg brain extract and dilutions thereof were also sufficient for the induction of Aβ deposition. Moreover, to sustain that Aβ in the Tg extract is key for the amyloid-inducing activity, Tg extract was mixed with an Aβ-specific antibody (β1) that has been shown previously to block seeding during intracerebral injection of the Tg extract (Meyer-Luehmann et al., 2006). The APP23 host was selected, and the inoculated mice survived for an 8 month incubation period. Results revealed that the one-time inoculation was comparable in all aspects with the inoculations separated by 1 week (Fig. 3 compared with Fig. 1). Although the 1:10 dilutions revealed approximately one-sixth of the induction observed with the undiluted extract, no detectable amyloid deposits were induced by the 1:100 and 1:1000 dilutions within the observation period, respectively (Fig. 3*C*). Strikingly, the 1:10 extract dilution induced predominantly vascular Aβ deposits (Fig. 3*B*,*F*), a phenomenon also observed in our previous study in intraperitoneally seeded APP23 Tg mice after 6–7 months of incubation (Eisele et al., 2010). Tg extract mixed with the β1 antibody primarily prevented amyloid induction (Fig. 3*A*,*B*), suggesting that the induction of cerebral β-amyloidosis is dependent on the concentration of Aβ seeds in the intraperitoneally inoculated Tg extract.

Distribution characteristics of the induced cerebral Aβ deposits

In APP23 mice, intraperitoneally induced cerebral Aβ deposits were much more abundant in the frontal cortex, followed by the entorhinal cortex, parietal cortex, hippocampus, and then other brain regions (Fig. 4*A*). This was also true for the R1.40 line (data not shown) matching the normal endogenous distribution of Aβ deposition in aged APP23 and R1.40 mice (Sturchler-Pierrat et al., 1997; Kulnane and Lamb, 2001).

Closer examination revealed that, for all intraperitoneally inoculated mice, independent of inoculation time and host line, there was appreciable clustering of parenchymal Aβ deposits throughout the brain (Fig. 4*B*). Typically large Aβ plaques, in most cases congophilic, were surrounded by a myriad of smaller Aβ deposits (Fig. 4*C*). On numerous occasions, vascular elements were observed in the center of the clusters.

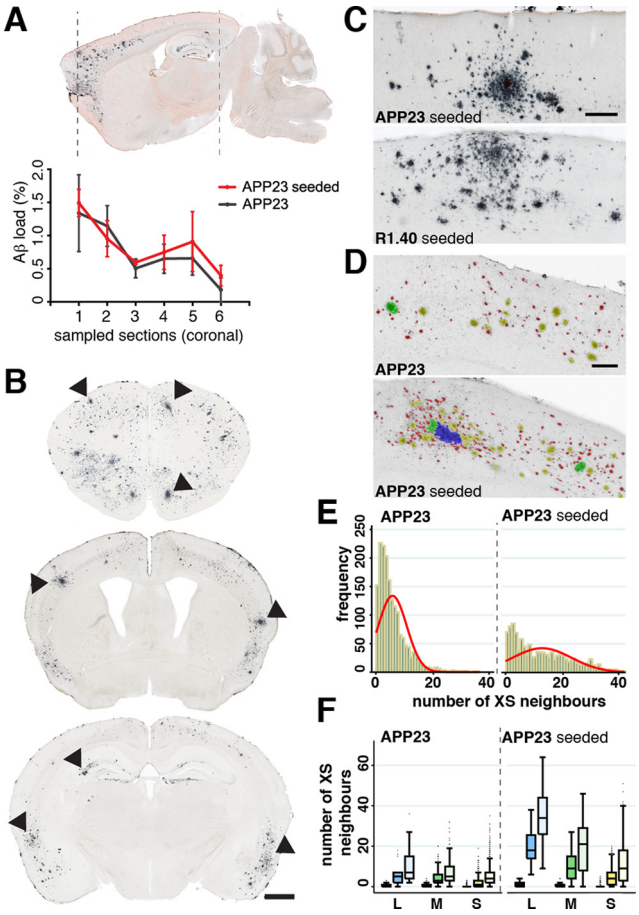

Figure 4. Regional distribution of intraperitoneally induced cerebral β-amyloidosis resembles endogenous amyloid deposition, albeit the induced amyloid deposits appear more clustered. ***A***, Intraperitoneally injected Aβ seeds predominantly induce Aβ deposits in the frontal cortex, followed by the parietal cortex and the hippocampus. Shown is a sagittal section of an APP23 mouse 8 months after the intraperitoneal inoculation. Stereological quantification of systematically sampled coronal sections (every 24th was taken) throughout the brain revealed a similar anterior-to-posterior distribution of plaque load in intraperitoneally seeded APP Tg mice compared with nonseeded APP23 Tg mice. For the analysis, five intraperitoneally seeded mice (7–8 months after inoculation; plaque load, 0.90 ± 0.09) were compared with five aged APP23 mice with a similar plaque load (12–14 months old; plaque load, 0.84 ± 0.25). Male and female mice were combined for the analysis (see Material and Methods). In the diagram, the mean ± SEM is shown. ***B***, Coronal sections through an APP23 Tg mouse brain intraperitoneally inoculated with Tg extract and incubated for 8 months. Note the clustering of the induced Aβ deposits (arrowheads). This is most evident in the posterior sections in which the induced amyloid load is less extensive compared with the anterior sections. Scale bar, 1000 μm. ***C***, Higher magnification of clustered Aβ deposits, in which typically a large plaque was surrounded by numerous smaller Aβ deposits. Shown is a representative image of an APP23 Tg mouse 8 months after inoculation and an R1.40 mouse 12 months after inoculation. ***D–F***, Quantitative analysis of clustering of Aβ deposits. Aβ deposits were quantified in size [blue for large (L), green for medium (M), yellow for small (S), and red for very small (XS)], and their *x–y* position was determined (for details, see Materials and Methods); an example is shown for the entorhinal cortex for intraperitoneally seeded and nonseeded APP23 Tg mice (***D***). The frequency distribution of the XS deposits (20–800 μm^2) around larger deposits (>800 μm^2), within 100 μm from their surface, revealed higher numbers of the XS deposits surrounding the larger Aβ deposits in intraperitoneally seeded APP23 Tg mice compared with nonseeded APP23 Tg mice (***E***). Differentiation between XS plaques surrounding L, M, and S plaques within 20, 50, and 100 μm from the surface yielded a significant increase in the number of XS neighboring plaques in intraperitoneally seeded APP23 Tg mice. However, the increase was most pronounced around the L and M plaques. Additionally, an increase of the number of neighbors around plaques of all sizes was evident in the intraperitoneally seeded animals as the distance to the plaque surface increased. The difference in the number of neighbors between nonseeded and seeded animals, for any plaque size, was significant ($p < 0.001$, Mann–Whitney test); darker-to-lighter box shading denotes 20, 50, and 100 μm from plaque surface, respectively, for each category (L, M, S); box hinges are 25th–75th percentiles, whiskers are adjacent values, and points are outliers. Scale bars: ***C***, ***D***, 200 μm.

To sustain this qualitative observation of clustering of the induced Aβ deposits, the localized distribution of Aβ deposits between intraperitoneally seeded and aged (nonseeded) APP23 Tg mice was investigated. A nearest-neighbor algorithm was applied on sections calculating the Euclidean distances between surfaces of plaques (Fig. 4*D–F*). The resulting quantification confirmed that, in intraperitoneally seeded APP23 mice, larger plaques had a substantially higher number of smaller plaques/Aβ deposits in their close vicinities compared with the endogenous plaques in nonseeded aged APP23 Tg mice (Fig. 4*D–F*).

Thus, despite the similar overall regional distribution of Aβ plaques throughout the brain, quantification of the microdistribution revealed more clustering of the amyloid deposits after intraperitoneal induction compared with aged nonseeded APP23 Tg mice.

Peripherally injected Aβ seeds are detectable shortly after injections in macrophages in the peritoneal cavity, blood, liver, and spleen

To get additional hints toward the mechanism by which intraperitoneally applied Aβ-containing brain material induces cerebral β-amyloidosis, APP23 mice were given single intraperitoneal injections of 200 μl of Tg or WT extract and killed within the first 24 h, one week, or 1 month after injection with subsequent analysis of the peritoneal cells, blood, peripheral organs, and brain.

Analysis of the cellular fraction isolated by peritoneal lavage by immunoassay revealed that ~2% of the injected human Aβ (Tg extract) could be recovered within peritoneal monocytes at 3 and 24 h after inoculation (Fig. 5*A*,*B*). After 1 week, some of the injected Aβ was still detectable (Fig. 5*A*,*B*). Similarly, human Aβ was detected in blood monocytes (CD11b and CD45 positive) in the Tg but not WT extract-injected mice, again peaking within the first 24 h after inoculation (Fig. 5*C–E*). In agreement, immunoblotting of the cellular blood fraction confirmed the presence of human Aβ (Fig. 5*F*). No change in blood plasma human Aβ levels was found at any examined time points (data not shown). Interestingly, Aβ taken up by peritoneal monocytes stained with the amyloid-specific dye pFTAA, indicating that at least some of it is aggregated and in β-sheet structure (Fig. 5*G*). Aβ-positive macrophages were also detected in the liver 1 d after the inoculation with the Tg extract (Fig. 5*H*) and only occasionally after 7 d. Aβ-positive staining of cellular and extracellular elements was found at 1 d after inoculation also in the spleen (data not shown). Consistent with previous work (Eisele et al., 2010), no Aβ deposition was found or induced in the examined peripheral tissues of APP23 mice (and also R1.40 mice) at 8 and 12 months after inoculation, respectively.

Discussion

We recently made the surprising observation that intraperitoneal inoculation of Aβ seed-containing brain extract induced cerebral β-amyloidosis in APP23 Tg mice (Eisele et al., 2010). A similar observation has just been described for Tau, i.e., the intraperitoneal administration of Tau aggregates was found to induce Tau lesions in Tau Tg mice (Clavaguera et al., 2014). In the present study, we further characterized the peripheral induction of cerebral β-amyloidosis and provide evidence for multiple brain entry sites of the Aβ seeds and self-propagation in brain. No evidence for peripheral amyloid formation was found even in mice expressing human APP systemically.

Intraperitoneal inoculation with Aβ-containing brain extract induced cerebral β-amyloidosis in all three APP Tg mouse lines used as hosts, i.e., APP23 mice, APP23 mice on *App*-null back-

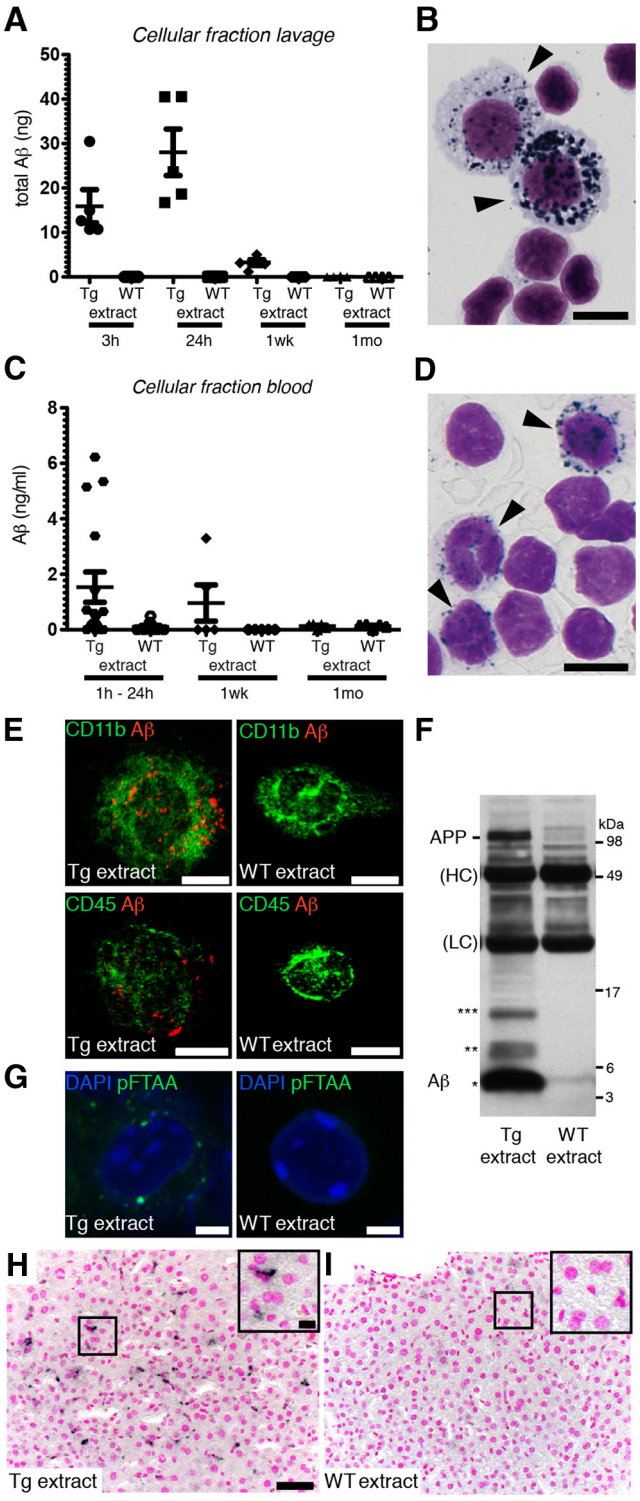

Figure 5. Intraperitoneally injected Aβ seeds are detectable shortly after the injection in macrophages in the peritoneal cavity, blood, liver, and spleen. ***A***, Electrochemiluminescence-conjugated immunoassay for human Aβ ($Aβ_{40}$ and $Aβ_{42}$ combined) in the cellular fraction of the peritoneal fluid 3 h, 24 h, 1 week, or 1 month after intraperitoneal inoculation with Tg or WT extract. Male or female 4- to 8-month-old APP23 mice, $n = 5$ per group and time point except $n = 4$ for the 1 month time point. Separate statistical analysis did not indicate a gender or age difference. ANOVA revealed significant main effects and a significant extract × post-inoculation time interaction ($F_{(3,30)} = 14.02$; $p < 0.001$). *Post hoc* Tukey's tests showed significantly more Aβ in the Tg extract-treated mice at 24 h compared with 3 h ($p < 0.05$) and 1 week ($p < 0.001$). Wilcoxon's comparisons revealed similar significances. Indicated is the mean ± SEM. ***B***, Pappenheim's stain (purple) combined with Aβ immunostaining (dark blue) of lavaged peritoneal cells from a Tg extract-inoculated mouse disclosed Aβ-positive monocytes (arrowheads). No Aβ immunoreactivity was found in WT extract-inoculated mice. ***C***, Electrochemiluminescence-conjugated immunoassay for human Aβ in the blood cellular fraction 1–24 h, 1 week, or 1 month after intraperitoneal inoculation. Male or female 4- to 8-month-old APP23 mice, $n = 16$ (Tg extract) and $n = 11$ (WT extract) for the 1–24 h time point and $n = 5$ per group for other time points. (Animals were added to the 1–24 h time period in an unsuccessful effort to reduce the high variability of Aβ measurements.) Separate statistical analysis did not indicate a gender or age difference. ANOVA indicated no significant differences, but Wilcoxon's test revealed a significant difference between Tg extract-treated and WT extract-treated mice in the 1–24 h post-inoculation group (median, 0.495 vs 0; $p < 0.05$). ***D***, Aβ-positive monocytes (arrowheads) in a blood film from a Tg extract-inoculated mouse (Pappenheim's stain, purple; Aβ immunostain, dark blue). ***E***, Double-immunofluorescence staining revealed that Aβ-positive (red) cells are positive for CD11b and CD45 (green; maximum projection of 10 μm *z*-stack). Scale bars, 10 μm. The same cells were also positive for CD68 (data not shown). ***F***, Immunoprecipitation of the blood cellular fraction with an antibody against human Aβ followed by immunoblot revealed a robust 4 kDa Aβ band in Tg extract-inoculated mice, as well as weaker oligomeric Aβ bands (indicated by asterisks) and APP, very similar as seen in the Tg extract (Langer et al., 2011). Only a weak signal corresponding to monomeric Aβ was seen in WT extract-inoculated mice, possibly because of residual human endogenous Aβ from the plasma fraction. IG heavy chain (HC) and light chain (LC) signals are attributable to coelution of the antibodies used for immunoprecipitation. ***G***, The amyloid-specific dye pFTAA stains Aβ in peritoneal monocytes isolated from Tg-extract inoculated mice. DAPI is used as a nuclear counterstain (scale bar, 5 μm). ***H***, ***I***, Peripheral organs of representative mice measured and stained in (***A–D***) were immunostained for Aβ and counterstained with nuclear fast red. Aβ-positive cells with the morphological characteristics of macrophages were found in the liver of Tg extract-inoculated mice ($n = 3$ analyzed mice) but not WT inoculated mice ($n = 2$ analyzed mice) 1 d after inoculation. Scale bar: 50 and 10 μm. In a separate study, non-Tg B6 mice were injected with Tg and WT extract ($n = 2$ for Tg and WT each) and analyzed 1 h, 1 d, 1 week, and 1 month later. Again, Aβ-positive cells with a macrophagic appearance were found after 1 and 7 d but not 1 month after inoculation (results not shown).

ground, and R1.40 mice (Lamb et al., 1997; Sturchler-Pierrat et al., 1997; Calhoun et al., 1999). Interestingly, the induction was earlier and stronger in APP23 than in R1.40 host. This is consistent with the approximate fivefold to sevenfold overexpression of human APP in the brain of APP23 mice (Sturchler-Pierrat et al., 1997) in contrast to the threefold overexpression of human APP in the R1.40 mice (Lamb et al., 1997). The result suggests that the availability of soluble Aβ peptides in brain plays a major role in the induction of cerebral amyloidosis by peripheral (intraperitoneal) inoculation of Aβ seeds. This is also supported by the observation that the peripherally induced amyloid distribution in brain reflected the endogenous distribution in both lines.

Mixing of antibody against Aβ to the brain extract before intraperitoneal injection greatly diminished induction of cerebral β-amyloidosis, and no induction was observed with intraperitoneally inoculated WT extract. These data are consistent with previous observations for intracerebral seeding (Meyer-Luehmann et al., 2006) and show that Aβ peptides are essential for the induction of cerebral β-amyloidosis in contrast to generalized reactions to the inoculation (e.g., inflammation, stress response). The present findings also indicate that relatively large amounts of Aβ seeds are needed to initiate cerebral β-amyloidosis by intraperitoneal seeding. Positive results were obtained after injection of extracts containing ~400 ng of total Aβ (1:10 dilution of Tg extract), indicating that intraperitoneal seeding is >1000-fold less potent than intracerebral seeding (Eisele et al., 2009; Langer et al., 2011). However, it should be noted that peritoneal inoculation starts plaque seeding in all cortical areas, whereas intracerebral seeding acts locally at the site of injection, e.g., the hippocampus or other brain regions (Eisele et al., 2009).

No induction of Aβ deposits in any peripheral tissue of the R1.40 mice was found despite the fact that R1.40 mice overexpress human APP in the periphery (Lamb et al., 1997). No amy-

loid induction in peripheral organs was also reported in APP23 mice (Eisele et al., 2010). Moreover, we observed efficient intraperitoneal seeding in APP23 mice on *App*-null background in which even peripheral mouse APP is missing. These data suggest that peripheral APP/Aβ expression may not be required for transmission of Aβ seeds from the peritoneal cavity to the brain. For Scrapie and other forms of transmissible spongiform encephalopathies or prion diseases, replication of misfolded PrP^{Sc} in peripheral tissues can occur before neuroinvasion (Brown et al., 1999) and play a major role in the prion spread throughout the infected organism (Aguzzi et al., 2013). In fact, peripheral PrP^{C} expression was found to be essential for clinical infection and transmission of Scrapie to the brain of mice (Blättler et al., 1997). However, more recently, diverse other routes have been reported depending on the concentration or nature (conformation) of the prions (Bett et al., 2012; Chen et al., 2014).

We aimed to follow the fate of the injected seeds and detected traces of the injected Aβ material in monocytes/macrophages in the peritoneal cavity, as well as in blood and tissue macrophages of liver and spleen shortly after injection. A significant decrease of this material was observed within 1 week, and it was below the detection limit at 1 month after inoculation. The uptake and degradation of Aβ aggregates by cells of the monocyte lineage is well documented (Majumdar et al., 2008; Zaghi et al., 2009; Lai and McLaurin, 2012; Michaud et al., 2013). We have shown recently that Aβ seeds are partly proteinase-K resistant (Langer et al., 2011), and insufficient clearance of Aβ seeds within cells has been shown to contribute to cell-to-cell spread of the seeds (Domert et al., 2014). These observations may explain the persistence of Aβ-immunoreactive monocytes for at least 1 week after intraperitoneal inoculation. Because peripheral phagocytes can be recruited to enter the brain (Rezai-Zadeh et al., 2011; Varvel et al., 2012) it is conceivable that they could serve to transport Aβ seeds from the periphery to the brain. However, it is also possible that Aβ seeds in blood plasma at levels below detection reach the brain (Mackic et al., 2002; Deane et al., 2003). Of note, it has been shown previously that AA amyloidosis can be transferred by blood monocytes (Sponarova et al., 2008).

A closer look at the distribution of the induced deposits revealed more clustering of intraperitoneally induced deposits compared with normally aged mice with similar amyloid load in APP23 Tg mice. This suggests that, in normally aged APP23 Tg mice, possibly because of the high overexpression of human APP, spontaneous aggregation occurs in many locations. In contrast, the pattern of Aβ aggregation in intraperitoneally seeded mice suggests hot spots of induction with subsequent spreading to areas in close proximity. It is tempting to speculate that the observed prominent vascular β-amyloidosis at early time points and with the 1:10 diluted extract reflects the route of transport of Aβ seeds. The formation of clusters may suggest that Aβ seeds enter the brain at various vascular locations in which local Aβ misfolding is initiated that subsequently spreads within the brain parenchyma. It is in agreement with the notion that corruptive templating of host Aβ occurs mainly in brain. Such a scenario may also explain why we found in our initial work a striking dominance of vascular amyloidosis after intraperitoneal inoculation (Eisele et al., 2010). It underlines that the nature and location of the induced Aβ deposits may vary with incubation time, Aβ seeds, and potentially also between host mice.

In summary, the peripheral induction of cerebral β-amyloidosis in APP Tg mice is dependent on the amount of inoculated Aβ-containing brain extract and on the level of APP/Aβ expression in the brain. No amyloid induction was found in peripheral organs. The induced Aβ deposits in brain occurred in a characteristic pattern consistent with the entry of Aβ seeds at multiple brain locations. Our results suggest that intraperitoneally inoculated Aβ seeds are transported from the periphery to the brain in which corruptive templating of host Aβ occurs at multiple sites, most efficiently in regions with high availability of soluble Aβ.

References

Aguzzi A, Nuvolone M, Zhu C (2013) The immunobiology of prion diseases. Nat Rev Immunol 13:888–902. CrossRef Medline

Bett C, Joshi-Barr S, Lucero M, Trejo M, Liberski P, Kelly JW, Masliah E, Sigurdson CJ (2012) Biochemical properties of highly neuroinvasive prion strains. PLoS Pathog 8:e1002522. CrossRef Medline

Blättler T, Brandner S, Raeber AJ, Klein MA, Voigtländer T, Weissmann C, Aguzzi A (1997) PrP-expressing tissue required for transfer of scrapie infectivity from spleen to brain. Nature 389:69–73. CrossRef Medline

Brown KL, Stewart K, Ritchie DL, Mabbott NA, Williams A, Fraser H, Morrison WI, Bruce ME (1999) Scrapie replication in lymphoid tissues depends on prion protein-expressing follicular dendritic cells. Nat Med 5:1308–1312. CrossRef Medline

Calhoun ME, Burgermeister P, Phinney AL, Stalder M, Tolnay M, Wiederhold KH, Abramowski D, Sturchler-Pierrat C, Sommer B, Staufenbiel M, Jucker M (1999) Neuronal overexpression of mutant amyloid precursor protein results in prominent deposition of cerebrovascular amyloid. Proc Natl Acad Sci U S A 96:14088–14093. CrossRef Medline

Chen B, Soto C, Morales R (2014) Peripherally administrated prions reach the brain at sub-infectious quantities in experimental hamsters. FEBS Lett 588:795–800. CrossRef Medline

Clavaguera F, Hench J, Lavenir I, Schweighauser G, Frank S, Goedert M, Tolnay M (2014) Peripheral administration of tau aggregates triggers intracerebral tauopathy in transgenic mice. Acta Neuropathol 127:299–301. CrossRef Medline

Colby DW, Prusiner SB (2011) Prions. Cold Spring Harb Perspect Biol 3:a006833. CrossRef Medline

Deane R, Du Yan S, Submamaryan RK, LaRue B, Jovanovic S, Hogg E, Welch D, Manness L, Lin C, Yu J, Zhu H, Ghiso J, Frangione B, Stern A, Schmidt AM, Armstrong DL, Arnold B, Liliensiek B, Nawroth P, Hofman F, Kindy M, Stern D, Zlokovic B (2003) RAGE mediates amyloid-beta peptide transport across the blood-brain barrier and accumulation in brain. Nat Med 9:907–913. CrossRef Medline

Domert J, Rao SB, Agholme L, Brorsson AC, Marcusson J, Hallbeck M, Nath S (2014) Spreading of amyloid-beta peptides via neuritic cell-to-cell transfer is dependent on insufficient cellular clearance. Neurobiol Dis 65C:82–92. CrossRef Medline

Eisele YS, Bolmont T, Heikenwalder M, Langer F, Jacobson LH, Yan ZX, Roth K, Aguzzi A, Staufenbiel M, Walker LC, Jucker M (2009) Induction of cerebral beta-amyloidosis: intracerebral versus systemic Abeta inoculation. Proc Natl Acad Sci U S A 106:12926–12931. CrossRef Medline

Eisele YS, Obermüller U, Heilbronner G, Baumann F, Kaeser SA, Wolburg H, Walker LC, Staufenbiel M, Heikenwalder M, Jucker M (2010) Peripherally applied Abeta-containing inoculates induce cerebral beta-amyloidosis. Science 330:980–982. CrossRef Medline

Hamaguchi T, Eisele YS, Varvel NH, Lamb BT, Walker LC, Jucker M (2012) The presence of Abeta seeds, and not age per se, is critical to the initiation of Abeta deposition in the brain. Acta Neuropathol 123:31–37. CrossRef Medline

Hefendehl JK, Neher JJ, Sühs RB, Kohsaka S, Skodras A, Jucker M (2014) Homeostatic and injury-induced microglia behavior in the aging brain. Aging Cell 13:60–69. CrossRef Medline

Jucker M, Walker LC (2013) Self-propagation of pathogenic protein aggregates in neurodegenerative diseases. Nature 501:45–51. CrossRef Medline

Kai H, Shin RW, Ogino K, Hatsuta H, Murayama S, Kitamoto T (2012) Enhanced antigen retrieval of amyloid beta immunohistochemistry: re-evaluation of amyloid beta pathology in Alzheimer disease and its mouse model. J Histochem Cytochem 60:761–769. CrossRef Medline

Kane MD, Lipinski WJ, Callahan MJ, Bian F, Durham RA, Schwarz RD, Roher AE, Walker LC (2000) Evidence for seeding of β-amyloid by intracerebral infusion of Alzheimer brain extracts in β-amyloid precursor protein-transgenic mice. J Neurosci 20:3606–3611. Medline

Kim JG, Keshava C, Murphy AA, Pitas RE, Parthasarathy S (1997) Fresh

mouse peritoneal macrophages have low scavenger receptor activity. J Lipid Res 38:2207–2215. Medline

Klingstedt T, Aslund A, Simon RA, Johansson LB, Mason JJ, Nyström S, Hammarström P, Nilsson KP (2011) Synthesis of a library of oligothiophenes and their utilization as fluorescent ligands for spectral assignment of protein aggregates. Org Biomol Chem 9:8356–8370. CrossRef Medline

Kulnane LS, Lamb BT (2001) Neuropathological characterization of mutant amyloid precursor protein yeast artificial chromosome transgenic mice. Neurobiol Dis 8:982–992. CrossRef Medline

Lai AY, McLaurin J (2012) Clearance of amyloid-beta peptides by microglia and macrophages: the issue of what, when and where. Future Neurol 7:165–176. CrossRef Medline

Lamb BT, Call LM, Slunt HH, Bardel KA, Lawler AM, Eckman CB, Younkin SG, Holtz G, Wagner SL, Price DL, Sisodia SS, Gearhart JD (1997) Altered metabolism of familial Alzheimer's disease-linked amyloid precursor protein variants in yeast artificial chromosome transgenic mice. Hum Mol Genet 6:1535–1541. CrossRef Medline

Langer F, Eisele YS, Fritschi SK, Staufenbiel M, Walker LC, Jucker M (2011) Soluble Abeta seeds are potent inducers of cerebral beta-amyloid deposition. J Neurosci 31:14488–14495. CrossRef Medline

Mabbott NA, MacPherson GG (2006) Prions and their lethal journey to the brain. Nat Rev Microbiol 4:201–211. CrossRef Medline

Mackic JB, Bading J, Ghiso J, Walker L, Wisniewski T, Frangione B, Zlokovic BV (2002) Circulating amyloid-beta peptide crosses the blood-brain barrier in aged monkeys and contributes to Alzheimer's disease lesions. Vascul Pharmacol 38:303–313. CrossRef Medline

Majumdar A, Chung H, Dolios G, Wang R, Asamoah N, Lobel P, Maxfield FR (2008) Degradation of fibrillar forms of Alzheimer's amyloid beta-peptide by macrophages. Neurobiol Aging 29:707–715. CrossRef Medline

Meyer-Luehmann M, Coomaraswamy J, Bolmont T, Kaeser S, Schaefer C, Kilger E, Neuenschwander A, Abramowski D, Frey P, Jaton AL, Vigouret JM, Paganetti P, Walsh DM, Mathews PM, Ghiso J, Staufenbiel M, Walker LC, Jucker M (2006) Exogenous induction of cerebral beta-amyloidogenesis is governed by agent and host. Science 313:1781–1784. CrossRef Medline

Michaud JP, Bellavance MA, Préfontaine P, Rivest S (2013) Real-time in vivo imaging reveals the ability of monocytes to clear vascular amyloid beta. Cell Rep 5:646–653. CrossRef Medline

Morales R, Duran-Aniotz C, Castilla J, Estrada LD, Soto C (2012) De novo induction of amyloid-beta deposition in vivo. Mol Psychiatry 17:1347–1353. CrossRef Medline

Radde R, Bolmont T, Kaeser SA, Coomaraswamy J, Lindau D, Stoltze L, Calhoun ME, Jäggi F, Wolburg H, Gengler S, Haass C, Ghetti B, Czech C, Hölscher C, Mathews PM, Jucker M (2006) Abeta42-driven cerebral amyloidosis in transgenic mice reveals early and robust pathology. EMBO Rep 7:940–946. CrossRef Medline

Rezai-Zadeh K, Gate D, Gowing G, Town T (2011) How to get from here to there: macrophage recruitment in Alzheimer's disease. Curr Alzheimer Res 8:156–163. CrossRef Medline

Rosen RF, Fritz JJ, Dooyema J, Cintron AF, Hamaguchi T, Lah JJ, LeVine H 3rd, Jucker M, Walker LC (2012) Exogenous seeding of cerebral beta-amyloid deposition in betaAPP-transgenic rats. J Neurochem 120:660–666. CrossRef Medline

Sponarova J, Nyström SN, Westermark GT (2008) AA-Amyloidosis can be transferred by peripheral blood monocytes. PLoS One 3:e3308. CrossRef Medline

Stöhr J, Watts JC, Mensinger ZL, Oehler A, Grillo SK, DeArmond SJ, Prusiner SB, Giles K (2012) Purified and synthetic Alzheimer's amyloid beta (Abeta) prions. Proc Natl Acad Sci U S A 109:11025–11030. CrossRef Medline

Sturchler-Pierrat C, Abramowski D, Duke M, Wiederhold KH, Mistl C, Rothacher S, Ledermann B, Bürki K, Frey P, Paganetti PA, Waridel C, Calhoun ME, Jucker M, Probst A, Staufenbiel M, Sommer B (1997) Two amyloid precursor protein transgenic mouse models with Alzheimer disease-like pathology. Proc Natl Acad Sci U S A 94:13287–13292. CrossRef Medline

Varvel NH, Grathwohl SA, Baumann F, Liebig C, Bosch A, Brawek B, Thal DR, Charo IF, Heppner FL, Aguzzi A, Garaschuk O, Ransohoff RM, Jucker M (2012) Microglial repopulation model reveals a robust homeostatic process for replacing CNS myeloid cells. Proc Natl Acad Sci U S A 109:18150–18155. CrossRef Medline

Watts JC, Giles K, Grillo SK, Lemus A, DeArmond SJ, Prusiner SB (2011) Bioluminescence imaging of Abeta deposition in bigenic mouse models of Alzheimer's disease. Proc Natl Acad Sci U S A 108:2528–2533. CrossRef Medline

Wilkinson M (1998) Segmentation techniques in image analysis of microbes, Chap 6. In: Digital image analysis of microbes: images, morphometry, fluorometry and motility techniques and applications (Wilkinson MHF, Schut F, eds). New York: Wiley.

Winkler DT, Bondolfi L, Herzig MC, Jann L, Calhoun ME, Wiederhold KH, Tolnay M, Staufenbiel M, Jucker M (2001) Spontaneous hemorrhagic stroke in a mouse model of cerebral amyloid angiopathy. J Neurosci 21:1619–1627. Medline

Zaghi J, Goldenson B, Inayathullah M, Lossinsky AS, Masoumi A, Avagyan H, Mahanian M, Bernas M, Weinand M, Rosenthal MJ, Espinosa-Jeffrey A, de Vellis J, Teplow DB, Fiala M (2009) Alzheimer disease macrophages shuttle amyloid-beta from neurons to vessels, contributing to amyloid angiopathy. Acta Neuropathol 117:111–124. CrossRef Medline